Proceedings of the XVII ECSMGE-2019
Geotechnical Engineering foundation of the future
ISBN 978-9935-9436-1-3

doi: 10.32075/17ECSMGE-2019-0899

XVII European Conference
ECSMGE 2019
Reykjavik
on Soil Mechanics
and Geotechnical Engineering

Numerical assessment of fragility curves for embankments on liquefiable ground

Évaluation numérique des courbes de fragilité des remblais sur sol liquéfiable

A. Oblak
University of Ljubljana, Faculty of Civil and Geodetic Engineering, Ljubljana, Slovenia

S. Kuder & J. Logar
University of Ljubljana, Faculty of Civil and Geodetic Engineering, Ljubljana, Slovenia

A. Viana Da Fonseca
CONSTRUCT-GEO, Faculty of Engineering, University of Porto (FEUP), Porto, Portugal

ABSTRACT: Fragility curves for highway and railway embankments have been developed for a set of ground conditions and different embankment heights and widths. Ground consisted of liquefiable layer underlain by competent base layer and covered by clayey crust. Numerical time history analyses were used with PM4sand material model as implemented in FLAC code. A set of 30 recorded ground motions was used, which were scaled to different peak ground accelerations.
Criteria for three levels of damage states for derivation of fragility curves for traffic embankments were taken from the literature. The influence of the position and thickness of the liquefiable layer, its properties and the influence of embankment geometry on the fragility curves will be presented.

RÉSUMÉ: Les courbes de fragilité des remblais routiers et ferroviaires ont été développées pour un ensemble de conditions de terrain et de différentes hauteurs et largeurs de remblais. Le sol consistait en une couche liquéfiable reposant sur une couche de base compétente et recouverte d'une croûte argileuse. Des analyses chronologiques numériques ont été utilisées avec le modèle de matériau PM4sand et implémenté dans le code FLAC. Un ensemble de 30 mouvements du sol enregistrés a été utilisé, qui ont été ajustés à différentes accélérations maximales du sol.
Les critères de trois niveaux d'état de dommage permettant de déduire les courbes de fragilité des remblais de circulation ont été repris de la littérature. L'influence de la position et de l'épaisseur de la couche liquéfiable, ses propriétés et l'influence de la géométrie du remblai sur les courbes de fragilité sont présentées.

Keywords: Liquefaction; Embankment; Fragility curve; FLAC

1 INTRODUCTION

In seismically active areas, where a soil profile is predominantly composed of loose sandy to silty sandy layers and saturated with groundwater, liquefaction can occur during seismic event. The occurrence of this phenomenon can cause serious damage to the infrastructure due to the increase of pore water pressure and consequent decrease of the shear strength in a soil medium.

Within this research a parametric study of an embankment built on a liquefiable ground was performed, upgraded with a probabilistic analysis to find the probability of exceedance of a selected damage states for road and railway embankments. For this purpose, a series of numerical models with advanced PM4Sand material model, capable of capturing dynamic behaviour of liquefiable soils, were simulated within FLAC software package. In order to decrease an influence of different uncertainties a set of 30 real ground motions with similar peak ground accelerations and various time durations were used for a seismic loading input.

Due to the complexity of soil liquefaction and its interaction with traffic embankment, a different failure mechanism at the surface of embankment can be found – crest settlements, slope instability, lateral spreading of the toe of the embankment, piping failure through cracks, water ponding on the road surface, etc. (Oka et al., 2012, Sasaki et al., 2007 and Argyroudis et al., 2018). According to aforementioned damage types, different engineering damage state parameter can be used for a construction of a fragility curve. Lagaros et al. (2009) constructed it based on a factor of safety, while Maruyama et al. (2010) used actual number of damage incidents per kilometre of expressway embankment, counted soon after four strong earthquake events in Japan (2003-2007). Nevertheless, crest settlements are still widely held as damage level, due to simple comparison with in-situ measurements from affected sites (Argyroudis and Kaynia, 2015, Khalil et al., 2017 and Argyroudis et al., 2018).

In the following sections a basic numerical model is presented (geometry, material characteristics, dynamic input, etc.) and the fragility curves for traffic embankments and other simulation outcomes are briefly described. In the conclusion, key findings are summarized.

2 DESCRIPTION OF THE NUMERICAL MODEL

For the purposes of this study, a simple numerical model consisting of a traffic embankment underlain by three horizontal soil layers was modelled in FLAC (Figure 1).

Under clayey crust layer, a sandy layer susceptible to liquefaction is placed, both underlain by base layer of stiff clay. Parametric study was made by varying thickness of liquefiable layer, embankment height, crest width and presence of crust layer. Ground water level, assigned one meter below the surface and embankment slope inclination equal to 1:2 (vertical:horizontal) were kept constant through all analyses. All geometry variations of the model are presented in section *2.1 Model geometry*.

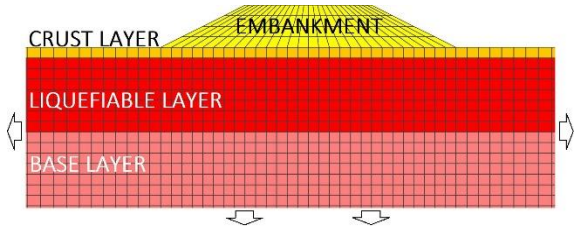

Figure 1. Basic numerical model in FLAC.

In order to satisfy accurate wave propagation through soil profile, the mesh density of finite difference model fulfilled the condition of spatial element size related to highest frequency component of input motion (FLAC manual, 2016). Moreover, the distance to the lateral boundary of the models increases by increasing the height of the embankment. Since a free field boundary condition in software packages cannot absorb all outward propagating waves, a sufficient width of the model ensures small enough influence on the behaviour of the embankment. At the bottom of the model, compliant base boundary condition was applied. Since we were only interested in embankment response during seismic loading (displacements and pore pressure build up), model displacement calculated at initial static condition phase, were zeroed before shaking.

2.1 Model geometry

The response of the embankment was observed on four different soil profiles (S1, S2, S4 and S5). Soil profile S1 and S2 contain 7 m thick liquefiable layer with 1 m of crust layer and without it, respectively. Whereas the thickness of the liquefiable layer, overlaid by crust layer (1 m), is smaller in soil profiles S4 (2 m) and S5 (4 m).

Initially, the models with different crest width (6 m, 12 m and 24 m) with four meters high embankment underlain by soil profile S1 were analysed. Subsequently, the various embankment heights (2 m, 4 m, 6 m and 8 m) were applied to all above soil profiles, where the crest width of the embankment remained constant and equal to 24 m.

2.2 Material properties

Table 1 contains material parameters used in numerical analyses.

Regardless of the model geometry, two sets of soil deposit properties were considered – with medium dense and loose sandy layer having $D_R = 0.60$ and $D_R = 0.35$, respectively. Material characteristics of crust and base layer were kept identical in all the analyses.

Same set of analyses in Figure 2 was repeated for both densities of liquefiable sandy layer.

Table 1. Material parameters used in FE analyses.

Layer	Dry density	Bulk modulus	Shear modulus	Undrained shear strength	φ'	c'	PM4Sand		
	(kg/m^3)	(MPa)	(MPa)	(kPa)	(°)	(kPa)	Dr (/)	G_0 (/)	h_{po} (/)
Crust	1784	64	30	80	-	-	-	-	-
Liquefiable "medium"	1486	77	77	-	30	0	0.60	760	0.55
Liquefiable "loose"	1486	57.3	43	-	30	0	0.35	476	0.5
Base	1436	227	105	150	-	-	-	-	-
Embankment	1800	83.3	38.5	-	35	5	-	-	-

All performed analyses are gathered in Figure 2.

Soil profile ID		Layer thickness [m]	Embankment height [m] (crest width: 24 m) 2	4	6	8
S1	Crust	1	✓	✓	✓	✓
	Liq.	7				
	Base	24				
S2	Crust	0	✓	✓	✓	
	Liq.	7				
	Base	24				
S4	Crust	1	✓	✓	✓	✓
	Liq.	2				
	Base	24				
S5	Crust	1	✓	✓	✓	✓
	Liq.	4				
	Base	24				

Figure 2. Matrix of performed analyses.

Note: Each tick inside the matrix in Figure 2 represents 240 analyses (30 ground motions multiplied by 8 intensity levels).

2.3 Input motions

30 ground motions recorded on rock outcrop with peak ground acceleration approximately 0.25 g were selected from the PEER database. The mean spectrum obtained from selected acceleration time histories coincides well with EC8 spectrum for soil class A. The duration of ground motions and Arias Intensity varies from 7.4 to 61.0 seconds (in average 17.4 seconds per ground motion) and 0.26 to 3.4, respectively. For the derivation of fragility curves, ground motions (transformed to shear stress history and applied to the compliant base of each model) were scaled to eight intensity levels (0.25 g, 0.375 g, 0.50 g, 0.625 g, 0.75 g, 1.00 g, 1.25 g and 1.50 g).

3 NUMERICAL FRAGILITY CURVES FOR EMBANKMENTS

The probability of exceedance of selected damage state (*ds*) for a given earthquake intensity measure (*IM*) is described through fragility functions. Two main parameters: median threshold value of *IM*, θ and total lognormal standard deviation, β are needed to develop the fragility curve. Usually, it is described by a lognormal cumulative distribution function, given by equation (1).

$$P_f(ds \geq ds_i|S) = \Phi\left[\frac{1}{\beta_{tot}} ln\left(\frac{IM}{IM_{mi}}\right)\right] \qquad (1)$$

where P_f is the probability that certain damage state for a given earthquake intensity measure is exceeded, Φ stands for standard cumulative probability function, IM_{mi} is the median threshold of intensity measure to cause *i*th damage state, and β_{tot} is the total lognormal standard deviation (Argyroudis et al., 2015).

Fragility curves within this research are based on correlation between damage states in terms of permanent vertical ground displacement in the middle of the embankment crest and PGA at bedrock as intensity measure.

The definitions of the limit states for traffic embankments were taken from literature and are presented in Table 2 and Table 3. For the evaluation of fragility curves, mean values of vertical displacement were used as threshold values for each damage state.

Table 2. Damage states for highway embankments (SYNER-G, 2013 - modified).

Damage state	**Permanent vertical ground displacement [m]**		
	min	max	**mean**
ds1 – minor	0.02	0.08	**0.05**
ds2 – moderate	0.08	0.22	**0.15**
ds3 – extensive	0.22	0.58	**0.40**

Table 3: Damage states for railway embankments (SYNER-G, 2013 - modified).

Damage state	**Permanent vertical ground displacement [m]**		
	min	max	**mean**
ds1 – minor	0.01	0.05	**0.03**
ds2 – moderate	0.05	0.10	**0.08**
ds3 – extensive	0.10	0.30	**0.20**

In terms of serviceability damage state "ds1" presents still useful road/railway with required speed reduction, while traffic is partially blocked for "ds2" and totally disabled during repair works for "ds3", respectively.

Figure 3 represents a sample of derivation of fragility curves based on calculated data from numerical analyses in FLAC. The fitting procedure, considering multiple IM levels was achieved using the maximum of likelihood function.

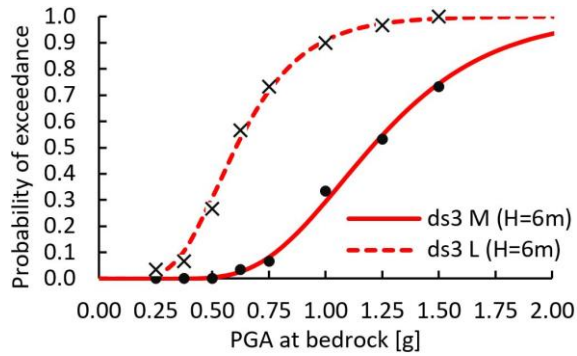

Figure 3. Observed data from FLAC and adjusted fragility curves.

In the figures (Figure 3 to 11), the light green colour depicts fragility curves for minor damage (ds1), the blue colour for moderate damage (ds2) and the red colour for extensive damage (ds3). Variation of crest width, embankment height, soil profiles and differentiation between cases with different relative density of liquefiable layer (L=loose and M=medium dense) are denoted by different line types and are additionally indicated in the legend of the figures.

3.1 Road embankments

3.1.1 Effect of crest width

Comparison was done on a case with soil profile S1 and for 4 m high embankment. Fragility curves presented in Figure 4 move to the right (vulnerability decreases) with increasing crest width for the studied range of crest widths (6 m, 12 m and 24 m).

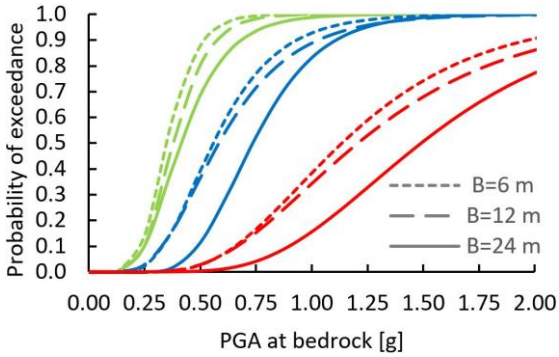

Figure 4. Fragility curves for different crest widths (road embankments) – ds1, ds2 & ds3.

3.1.2 Effect of embankment height

For this comparison, embankment with 24 m wide crest and built on soil profile S1 was analysed. Figure 5 expresses higher influence of embankment height on fragility curves than crest width, especially for extensive damage state (ds3). The higher the embankment, the higher are crest settlements.

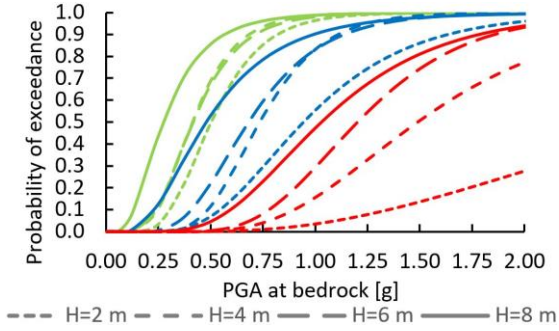

Figure 5. Fragility curves for different embankment height (road embankments) – ds1, ds2 & ds3.

3.1.3 Effect of thickness of liquefiable layer

Fragility curves in Figure 6 are based on results of numerical analyses, where embankment height was 4 m and crest width 24 m. Expectedly, thickness of liquefiable layer has great impact on soil/embankment response. Crest settlements increase and consequently fragility curves move to the left with increasing thickness of liquefiable layer (2 m, 4 m and 7 m). Even larger settlements were calculated in case without crust layer and with 7 m thick liquefiable layer. Reliability of fragility curves for soil profile S5 and S4 for extensive damage state is very low, due to the lack of calculations where the embankment is subjected to more intense ground motions.

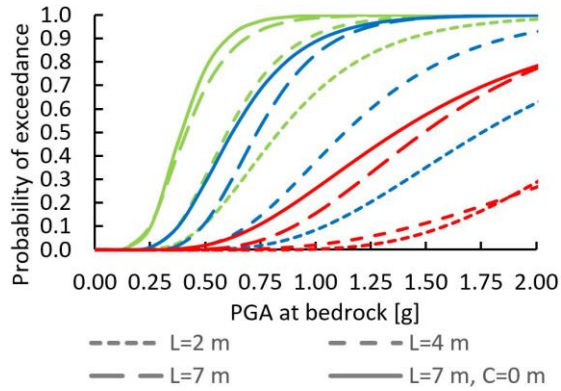

Figure 6. Fragility curves for different soil profiles (road embankments) – ds1, ds2 & ds3.

3.1.4 Comparison between "loose" and "medium dense" case

Effect of soil density of the liquefiable layer is captured through fragility curves in Figure 7. The results of the models with S1 soil profile, 4 m high embankment and 24 m wide crest were examined.

A greater potential for liquefaction and larger deformations of the embankment are expected for ground profile with loose sand, which is also confirmed by fragility curves in Figure 7.

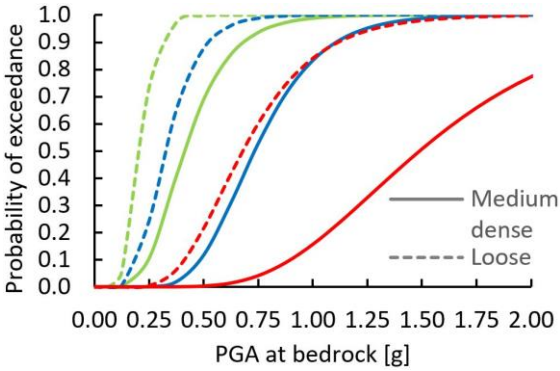

Figure 7. Fragility curves for different relative density in liquefiable sandy layer (road embankments) – ds1, ds2 & ds3.

3.2 Railway embankments

Similar trends were obtained for railway embankments. However, all fragility curves for railway embankments are shifted to the left in relation to fragility curves for road embankments, due to more strict damage state criteria. Also the slope of some curves (e.g. dashed curve for minor damage (ds1) in Figure 11) changed drastically, which indicates that some damage states are exceeded instantly. Better results will be achieved with smaller steps of intensity measure.

The effects of variations of the model geometry and material properties for liquefiable layer, expressed through fragility curves related to limit states for railway embankments, are gathered in figures below (Figure 8 to 11).

3.2.1 Effect of crest width

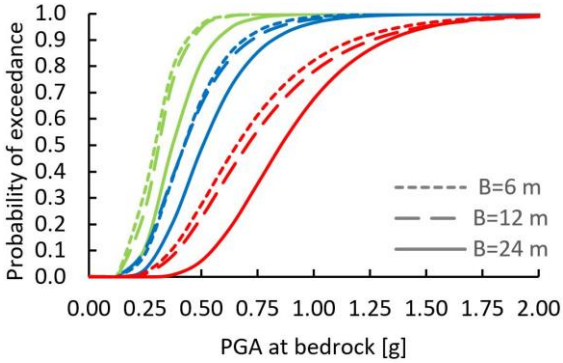

Figure 8. Fragility curves for different crest width (railway embankments) – ds1, ds2 & ds3.

3.2.2 Effect of embankment height

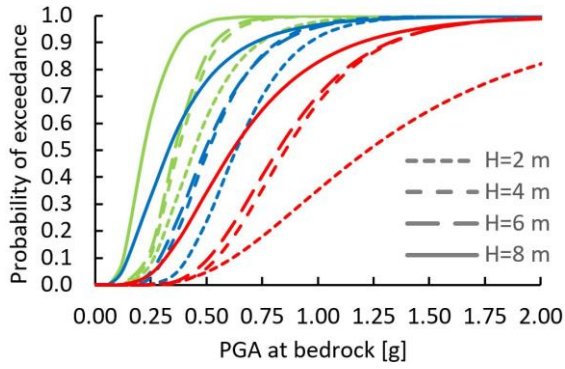

Figure 9. Fragility curves for different embankment height (railway embankments) – ds1, ds2 & ds3.

3.2.3 Effect of thickness of liquefiable layer

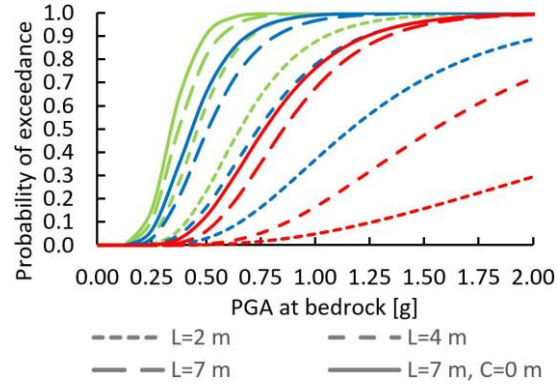

Figure 10. Fragility curves for different soil profiles (railway embankments) – ds1, ds2 & ds3.

3.2.4 Comparison between "loose" and "medium dense" case

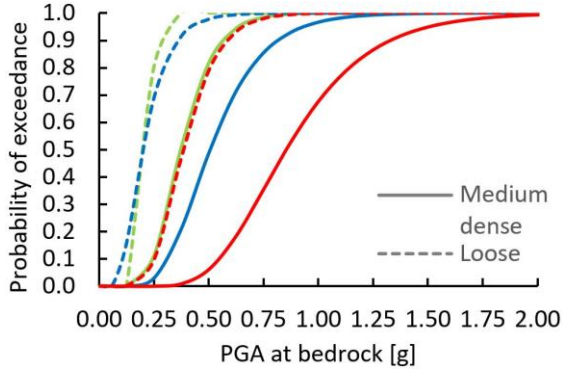

Figure 11. Fragility curves for different relative density in sandy layer (railway embankments) – ds1, ds2 & ds3.

4 CREST DEFORMATION SHAPE

Although a set of 30 ground motions for each analysis were used to take account of variability of earthquake input data, a large amount of uncertainties remains due to the definition of damage states, which is especially challenging task in geotechnics, due to the soil diversity.

Besides threshold values of the limit states, the location of the observed point(s) is also important. From Figure 12, representing a deformed shapes of the embankment crest, it is evident that middle point is representative for the case B = 6 m, while for B = 24 m the choice of a representative point is a matter of discussion. Both curves were obtained with same input data, except crest width. A detailed exploration of all performed analyses exceeds the scope of this paper.

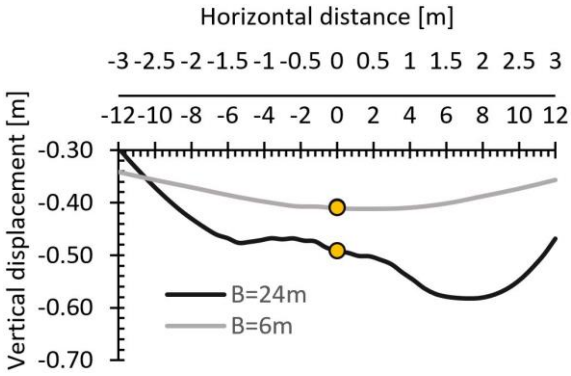

Figure 12. Crest deformation shapes for crest width B = 6 m and B = 24 m.

5 CONCLUSIONS

An extensive study of the earthquake-liquefaction-induced deformations of the traffic embankments was conducted within this work. Numerical analyses were carried out with 2D finite element code FLAC, using advanced PM4Sand material model to capture soil behaviour during seismic event. The influence of variation of some model parameters (crest width, embankment height, thickness of liquefiable layer, presence of crust layer and relative density of sandy layer) was examined through fragility curves. A set of 30 ground motions was used to prepare fragility curves, where permanent vertical ground displacement in the middle point of embankment crest was used as damage parameter and PGA at bedrock for intensity measure. Based on the above figures, the following was found:

- With increasing embankment height (2 m, 4 m, 6 m and 8 m) or thickness of liquefiable layer (2 m, 4 m, and 7 m) crest settlements increase and fragility curves move to the left. In the absence of crust layer even higher probability of exceedance of the damage state was observed.
- The increase of crest width (6 m, 12 m and 24 m) decreases vertical displacement in the centre of the embankment crest. Fragility curves move to the right with larger crest width.
- Denser liquefiable layer produces smaller deformations at the crest in comparison with loose material. Consequently, fragility curves move to the left for cases with loose sand.

Fragility curves were prepared for road and railway embankments based on SYNER-G criteria (SYNER-G, 2013). Similar conclusions can be made for road and railway embankments with expected differences due to more strict damage state criteria for railway embankments.

Finally, the problem of uncertainties regarding the damage states for traffic embankments, and geostructures in general was presented.

6 ACKNOWLEDGEMENTS

This paper is produced as part of the LIQUEFACT project (“Assessment and mitigation of liquefaction potential across Europe: a holistic approach to protect structures / infrastructures for improved resilience to earthquake-induced liquefaction disasters”) and has received funding from the European Union's Horizon 2020 research and innovation programme under grant agreement No GAP-700748.

7 REFERENCES

Argyroudis, S., Kaynia, A. M. 2015. Analytical seismic fragility functions for highway and railway embankments and cuts, Earthquake Engineering & Structural Dynamics **44**, 1863-1879.

Argyroudis, S., Mitoulis, S., Kaynia, A. M., Winter, M. G. 2018. Fragility Assessment of Transportation Infrastructure Systems Subjected to Earthquakes, Geotecnical Earthquake Engineering and Soil Dynamics V GSP 292, 174-183.

FLAC manual, 6th ed. Itasca Consulting Group Inc., Minneapolis, Minesota, USA, February 2016, pp. 48.

Khalil, C., Rapti, I., Lopez-Caballero, F. 2017. Numerical Evaluation of Fragility Curves for Earthquake-Liquefaction-Induced Settlements of an Embankment, Geo-Risk 2017 GSP 283, 21-30.

Lagaros, N. D., Tsompanakis, Y., Psarropoulus, P. N., Georgopoulos, E. C. 2009. Computationally efficient seismic fragility analysis of geostructures, Computers and Structures **87**, 1195-1203.

Maruyama, Y., Yamazaki, F., Mizuno, K., Tsuchiya, Y., Yogai, H. 2010. Fragility curves for expressway embankments based on damage datasets after recent earthquakes in Japan, Soil Dynamics and Earthquake Engineering **30**, 1158-1167.

Oka, F., Tsai, P., Kimoto, S., Kato, R. 2012. Damage patterns of river embankments due to the 2011 off the Pacific Coast of Tohoku Earthquake and a numerical modeling off the deformation of river embankments with a clayey subsoil layer, Soils and Foundations **52(5)**, 890-909.

Sasaki, Y., Tamura, K. 2007. Failure mode of embankments due to recent earthquakes in Japan, 4th International Conference on Earthquake Geotechnical Engineering, Thessaloniki, Greece, 1479.

SYNER-G fragility curves for all elements at risk. 2013. Kaynia, M. A. (ed.). Systemic Seismic Vulnerability and Risk Analysis for Buildings, Lifeline Networks and Infrastructures Safety Gain. Project N°: 244061, Call N°: FP7-ENV-2009-1.